

1 **The chromatin remodeling factor SPOC1 acts as a cellular restriction**
2 **factor against human cytomegalovirus by repressing the major**
3 **immediate-early promoter**

4 Anna Reichel^a, Anne-Charlotte Stilp^a, Myriam Scherer^b, Nina Reuter^a, Sören Lukassen^c,
5 Bahram Kasmapour^e, Sabrina Schreiner^d, Luka Cicin-Sain^{e,f,g}, Andreas Winterpacht^c, and
6 Thomas Stamminger^{b§}

7

8 ^aInstitute for Clinical and Molecular Virology, Friedrich-Alexander-Universität Erlangen-
9 Nürnberg, Erlangen, Germany

10 ^bInstitute of Virology, Ulm University Medical Center, Ulm, Germany

11 ^cInstitute for Human Genetics, Friedrich-Alexander-Universität Erlangen-Nürnberg,
12 Erlangen, Germany

13 ^dInstitute of Virology, Technical University of Munich/Helmholtz Zentrum München,
14 Munich, Germany

15 ^eDepartment of Vaccinology and Applied Microbiology, Helmholtz Centre for Infection
16 Research, Braunschweig, Germany

17 ^fInstitute for Virology, Hannover Medical School, Hannover, Germany

18 ^gGerman Centre for Infection Research (DZIF), Site Hannover/Braunschweig, Germany

19 Running title: SPOC1 restricts HCMV IE gene expression

20 [§]corresponding author: phone: +49 731-50065100, fax: +49 731-50065102, e-mail:

21 thomas.stamminger@uniklinik-ulm.de

22 Word count of abstract: 249; Word count of text: 7237

23 **ABSTRACT**

24 The cellular protein SPOC1 (survival time-associated PHD finger protein in ovarian cancer
25 1) acts as a regulator of chromatin structure and DNA damage response. It binds
26 H3K4me2/3 containing chromatin and promotes DNA condensation by recruiting
27 corepressors such as KAP-1 and H3K9 methyltransferases. Previous studies identified
28 SPOC1 as a restriction factor against human adenovirus (HAdV) infection that is
29 antagonized by E1B-55K/E4orf6-dependent proteasomal degradation. Here, we
30 demonstrate that, in contrast to HAdV-infected cells, SPOC1 is transiently upregulated
31 during the early phase of HCMV replication. We show that expression of the immediate-
32 early protein 1 (IE1) is sufficient and necessary to induce SPOC1. Additionally, we
33 discovered that during later stages of infection SPOC1 is downregulated in a GSK-3 β -
34 dependent manner. We provide evidence that SPOC1 overexpression severely impairs
35 HCMV replication by repressing the initiation of viral immediate early (IE) gene
36 expression. Consistently, we observed that SPOC1-depleted primary human fibroblasts
37 displayed augmented initiation of viral IE gene expression. This occurs in a MOI-
38 dependent manner, a defining hallmark of intrinsic immunity. Interestingly, repression
39 requires the presence of high SPOC1 levels at the start of infection while a later
40 upregulation had no negative impact suggesting distinct temporal roles of SPOC1 during
41 the HCMV replicative cycle. Mechanistically, we observed a highly specific association of
42 SPOC1 with the major immediate-early promoter (MIEP) strongly suggesting that SPOC1
43 inhibits HCMV replication by MIEP binding and subsequent recruitment of
44 heterochromatin building factors. Thus, our data add SPOC1 as a novel factor to the
45 endowment of a host cell to restrict cytomegalovirus infections.

46 **IMPORTANCE**

47 Accumulating evidence indicates that during millennia of co-evolution host cells have
48 developed a sophisticated compilation of cellular factors to restrict cytomegalovirus
49 infections. Defining this equipment is important to understand cellular barriers against viral
50 infection and to develop strategies to utilize these factors for antiviral approaches. So far,
51 constituents of PML nuclear bodies and the interferon gamma inducible protein 16 (IFI16)
52 were known to mediate intrinsic immunity against HCMV. In this study, we identify the
53 chromatin modulator SPOC1 as a novel restriction factor against HCMV. We show that
54 pre-existing high SPOC1 protein levels mediate a silencing of HCMV gene expression via
55 a specific association with an important viral *cis*-regulatory element, the major immediate-
56 early promoter. Since SPOC1 expression varies between cell-types, this factor may play
57 an important role in the tissue-specific defense against HCMV.

58 **INTRODUCTION**

59 Restriction factors represent a front line defense against viral infections (1). They
60 constitute the basis of intrinsic antiviral immunity, which is either considered as part of the
61 innate immune response, or as an independent, third branch of the immune system. One
62 characteristic of these factors is their constitutive expression within the host cell allowing
63 for a rapid response to viral infection that precedes the interferon response. The best
64 characterized restriction factors targeting human cytomegalovirus (HCMV) are cellular
65 constituents of the nuclear domain 10 (ND10), also called PML (promyelocytic leukemia
66 protein) nuclear bodies, and the interferon gamma inducible protein 16 (IFI16) (2, 3).
67 Previous studies demonstrated that several ND10 components exert their antiviral activity
68 independently by inducing a transcriptionally inactive chromatin state around the major
69 immediate-early promoter (MIEP) which leads to a silencing of viral IE gene expression
70 (2, 4-12). IFI16 was shown to downregulate transcription of the viral DNA polymerase
71 pUL54, which results in an inhibition of viral DNA synthesis (3). An additional hallmark
72 of restriction factors is the fact that they are saturable and subject to viral countermeasures.
73 During co-evolution with its host, HCMV has evolved regulatory proteins, such as the
74 tegument proteins pp71, pp65 and pUL97, as well as the immediate-early protein 1 (IE1)
75 to counteract the antiviral activity of ND10 factors and IFI16 in order to efficiently initiate
76 lytic replication (2, 10, 11, 13-19).

77 SPOC1 (survival time-associated PHD protein in ovarian cancer 1), also known as
78 PHF13 (PHD finger 13), was first described in 2003 as a novel cellular protein with a single
79 PHD domain and enhanced SPOC1 transcript levels were demonstrated to correlate with a
80 shorter survival time in patients suffering from epithelial ovarian cancers (20).

81 Subsequently, this cellular protein has been associated with several functions in cell
82 biology such as the modulation of cellular proliferation and spermatogenesis, which was
83 attributed to at least three different mechanisms. One proposed mechanism involves the
84 interaction of SPOC1 with chromatin which occurs in a multivalent fashion. On the one
85 hand, it harbors a C-terminally located PHD domain (plant homeodomain), which serves
86 as a molecular reader of the histone marker H3K4me2/3 (21-23). Upon binding to
87 H3K4me2/3, SPOC1 was proposed to induce chromatin compaction by recruiting histone
88 methyl transferases (HMTs), such as SETDB1, G9A or GLP, subsequently resulting in an
89 increase of repressive H3K9me3 (24). On the other hand, there is recent evidence that a
90 centrally located domain enables an interaction of SPOC1 with DNA, which contributes to
91 its chromatin binding avidity (23). While SPOC1 is able to directly bind to chromatin, it
92 was also shown to contact chromatin indirectly by interacting with several heterochromatin
93 proteins. In this respect, Chung and colleagues postulated that SPOC1 acts as a
94 transcriptional co-regulator, by functioning as a scaffolding protein or bridging factor for
95 recruitment of RNA polymerase II (RNAPII) complexes as well as Polycomb repressive
96 complex 2 (PRC2) to distinct chromatin landscapes. The authors suggested that SPOC1
97 thereby differentially regulates subsets of target genes that were found to mainly function
98 in DNA binding and chromatin organization as well as transcription, cell cycle regulation,
99 and differentiation (23). Besides transcriptional co-regulation and chromatin compaction,
100 SPOC1 was also demonstrated to modulate DNA repair as it is recruited to DNA double
101 strand breaks (DSBs) in an ATM-dependent manner and regulates the kinetics of DNA
102 damage repair (DDR). Thereby, SPOC1 is able to shift the balance between non-
103 homologous end joining (NHEJ) and homologous recombination (HR) favoring HR (24).

104 Apart from its cellular regulatory functions, SPOC1 was also implicated to
105 contribute to the intrinsic defense against viral infections (25). First evidence for this was
106 presented by Schreiner and colleagues demonstrating that human adenovirus type 5
107 (HAdC5) infection was diminished at the transcriptional level when SPOC1 was
108 overexpressed, while its depletion resulted in increased virus titers. Furthermore, they
109 showed that the HAdV E3 ubiquitin ligase complex E1B-55K/E4orf6 efficiently
110 antagonizes SPOC1 by inducing its proteasomal degradation early after infection.
111 Interestingly, recent reports suggest that SPOC1 plays a dual role during HIV-1 infection
112 (26). Depending on the time point of HIV-1 replication, high SPOC1 levels either improved
113 HIV-1 integration (SPOC1 expression prior to HIV-1 integration), or suppressed viral gene
114 expression (SPOC1 expression post HIV-1 integration). Furthermore, the authors
115 demonstrated that the viral accessory protein Vpr counteracts SPOC1 by targeted
116 degradation (26).

117 Here, we analyzed the role of SPOC1 in the context of HCMV infection.
118 Intriguingly, and in contrast to HAd and HIV-1 infection, we observed that SPOC1
119 expression is upregulated during infection and peaks during the early phase of the HCMV
120 replicative cycle. Furthermore, we could show that at late times post infection, SPOC1 is
121 degraded in a GSK-3 β -dependent manner. In order to elucidate the role of SPOC1 during
122 HCMV infection, we generated SPOC1 overexpressing fibroblasts and observed severely
123 impaired virus growth at low MOI. Furthermore, we show that overexpression of SPOC1
124 restricts the onset of viral IE gene expression while its depletion results in an increase of
125 IE gene expression. Finally, by ChIPseq analyses we demonstrate a specific association of

- 126 SPOC1 with the HCMV MIEP region strongly arguing for a scenario whereby SPOC1 is
127 able to induce a silencing of viral IE expression via epigenetic modifications.

128 **MATERIAL AND METHODS**

129 **Oligonucleotides and plasmid constructions.** The oligonucleotide primers used for this
130 study were purchased from Biomers GmbH (Ulm, Germany) or Biomol (Hamburg,
131 Germany) and are listed in [Table 1](#). The lentiviral construct pHM4300 for stable SPOC1
132 overexpression was generated by amplification using the FLAG-tagged *SPOC1* plasmid
133 pCMV-Flag-SPOC1 (provided by A. Winterpacht, Erlangen, Germany) and primers
134 SPOC1_PacI_fw and SPOC1_EcoRI_rev, followed by insertion via *PacI* and *EcoRI* into
135 a modified pLKO-based lentiviral vector. The modified pLKO-based lentiviral vector was
136 generated beforehand as described elsewhere (27). For inducible expression of SPOC1,
137 FLAG-tagged SPOC1 was generated by PCR amplification with primers F-SPOC1_NotI
138 and SPOC1_EcoRI_rev along with pCMV-Flag-SPOC1 as the template, followed by
139 insertion into the lentiviral pLVX-Tight-Puro vector via *NotI* and *EcoRI*. The modified
140 pLVX Tet-On Advanced was generated by substitution of the CMV promoter with an EF1-
141 alpha promoter by amplification of EF1-alpha promoter sequences with primers EF1-
142 alpha_ClaI_fw and 3'EF1alpha-BamHI using pHM4300 as template, followed by insertion
143 into the pLVX Tet-On Advanced via *ClaI* and *BamHI*. The SPOC1 guide RNA primers
144 SPOC1-fw-gRNA and SPOC1-rev-gRNA were designed with <http://crispr.mit.edu/>,
145 annealed and cloned into the pLenti-CRISPR-v2 vector (kindly provided by A. Ensser,
146 Erlangen, Germany) via *BsmBI* (28).

147 **Cells and viruses.** HEK293T cells were cultivated in Dulbecco's minimal essential
148 medium (DMEM) (Gibco, Thermo Fisher Scientific, Waltham, MA, USA) containing 10%
149 fetal calf serum (FCS). Primary human foreskin fibroblasts (HFFs) and human retinal

150 pigment epithelial cells (ARPE-19) were maintained in Eagle's minimal essential medium
151 (MEM) (Gibco, Thermo Fisher Scientific, Waltham, MA, USA) supplemented with 7 %
152 fetal calf serum. Mouse embryonic fibroblasts (MEFs) were cultivated with DMEM
153 supplemented with 10 % fetal calf serum. HFFs stably overexpressing SPOC1 and
154 respective control cells were maintained in MEM supplemented with 7 % fetal calf serum
155 and 500 µg/ml geneticin. HFFs with a stable *SPOC1* knockout were maintained in MEM
156 supplemented with 10% fetal calf serum and 5 µg/ml puromycin. HFF cells with inducible
157 overexpression of FLAG-tagged SPOC1 were cultured in MEM supplemented with 10%
158 tetracycline-free fetal bovine serum (Clontech, Palo Alto, CA, USA), 5 µg/ml puromycin
159 and 500 µg/ml geneticin. Infection experiments in HFFs were performed with the HCMV
160 laboratory strain AD169, the recombinant viruses AD169/IE1-L174P and AD169ΔIE1 and
161 the clinical isolate TB40/E (29, 30). UV-inactivated AD169 was generated by exposure of
162 wild-type AD169 to UV light (0.12 J/cm²). The used recombinant reporter HCMV strain
163 TB40/E-IE-mNeonGreen was generated as described elsewhere (31). One day prior to
164 infection HFF cells were seeded into six-well dishes (3×10⁵ cells/well). Virus inoculation
165 was carried out at the specified multiplicities of infection (MOIs) and cells were provided
166 with fresh medium 1.5 hours post infection (hpi) before using them for subsequent
167 analyses. Viral stocks were titrated as described elsewhere (29). Infection of ARPE-19 cells
168 was performed one day after seeding into six-well dishes (4.5×10⁵ cells/well). In contrast
169 to HFFs, ARPE-19 cells were inoculated with 2 ml of TB40/E and centrifuged at 1200 rcf
170 for 30 min at 37 °C and provided with fresh medium 1.5 hpi. For MCMV infection MEF

171 cells were seeded into six-well dishes (1×10^5 cells/well) and one day later inoculated with
172 MCMVlucMCK2 (kindly provided by M. Mach, Erlangen, Germany) (32).

173 **Lentivirus transduction and selection of stably transduced cells.** For the generation of
174 HFF/control and HFF/SPOC1 cells replication-deficient lentiviruses were generated using
175 pLKO-based expression vectors. For this purpose, HEK293T cells were seeded in 10-cm
176 dishes (5×10^6 cells) cotransfected with an empty pLKO vector or one encoding for *SPOC1*
177 together with packaging plasmids pLP1, pLP2, and pLP/VSV-G using the Lipofectamine
178 2000 reagent (Invitrogen, Karlsruhe, Germany). Viral supernatants were harvested 48 h
179 post transfection, cleared by centrifugation, filtered, and stored at -80°C . HFFs of low
180 passage number were incubated for 24 h with lentiviral supernatants in the presence of 7.5
181 $\mu\text{g/ml}$ polybrene (Sigma-Aldrich, St. Louis, MO, USA). Stably transduced HFF cell
182 populations were selected by addition of 500 $\mu\text{g/ml}$ geneticin to the cell culture medium.
183 *SPOC1* knockout HFFs were generated in an analogous fashion, using the empty
184 pCRISPRv2 vector or the *SPOC1* gRNA-encoding plasmid pHM4395 for production of
185 lentiviral supernatants. However, selection of successfully transduced HFF populations
186 was performed by addition of 5 $\mu\text{g/ml}$ puromycin to cell culture media. The Lenti-X Tet-
187 On Advanced Inducible Expression System (Clontech, Palo Alto, CA, USA) was used to
188 generate HFFs with an inducible overexpression of FLAG-tagged SPOC1. Therefore,
189 replication-deficient lentiviruses expressing the modified tetracycline-controlled
190 transactivator rtTA-Advanced were generated by cotransfecting HEK293T cells with the
191 modified pLVX-Tet-On Advanced vector and the Lenti-X HTX packaging mix (Clontech,
192 Palo Alto, CA, USA), while lentiviruses expressing *SPOC1* under the control of the

193 inducible pTight promoter were generated by cotransfection with the pLVX-Tight-Puro
194 vector. Respective viral supernatants were harvested 48 h after transfection, cleared by
195 centrifugation, filtered, and subsequently used for co-transduction of primary HFFs
196 followed by selection with 500 $\mu\text{g/ml}$ geneticin and 5 $\mu\text{g/ml}$ puromycin. HFFs with
197 inducible expression of IE1 were generated as described elsewhere (29).

198 **Western blotting, indirect immunofluorescence and antibodies.** Whole-cell lysates
199 from HFF, ARPE-19, HEK293T or MEF cells were prepared in Roti-Load Laemmli buffer
200 (Roth GmbH, Karlsruhe, Germany) and boiled for 10 min at 95°C (33). Proteins were
201 separated by SDS-PAGE (SDS-polyacrylamide gel electrophoresis) on 8% to 12.5%
202 polyacrylamide gels and transferred onto nitrocellulose membranes (GE Healthcare,
203 Munich, Germany), subsequent chemiluminescence detection was performed according to
204 the manufacturer's instructions (ECL Western blotting detection kit; Amersham Pharmacia
205 Europe, Freiburg, Germany). For indirect immunofluorescence analysis the transduced
206 HFFs were fixed with 4 % paraformaldehyde and fluorescence staining was performed as
207 described elsewhere (34). A Leica TCS SP5 confocal microscope with 488-nm and 543-nm
208 laser lines was used for subsequent sample analysis, where each channel was scanned
209 separately under image capture conditions thereby eliminating channel overlap. The
210 images were then exported, processed with Adobe Photoshop CS5, and assembled using
211 CorelDraw X5. The following monoclonal antibodies were used for immunofluorescence
212 and Western blot analyses: α -SPOC1 rat, α -IE1 p63-27, α -UL44 BS510 (kindly provided
213 by B. Plachter, Mainz, Germany), α -UL97 (kindly provided by M. Marschall, Erlangen),
214 α -pp65 65-33 (kindly provided by W. Britt, Birmingham, USA), α -pp28 41-18, α -MCP 28-

215 4, α -mouse gB 5F12 kindly provided by M. Mach, Erlangen, α -FLAG 1804, α -HA clone 7
216 and α - β -actin AC-15 (Sigma-Aldrich, Deisenhofen, Germany) (22, 32, 35-38). The
217 following polyclonal antibodies were used for immunofluorescence and Western blot
218 analyses: α -SPOC1-rabbit CR54; α -IE2 pHM178 (produced by immunizing rabbits with
219 prokaryotically expressed protein); α -UL84; α -pp71 SA2932, α -PML A301-167A in
220 combination with α -PML A301-168A (Bethyl Laboratories), α -GSK-3 β H-76 (Santa Cruz
221 Biotechnology, Heidelberg, Germany) (5, 22, 39). Horseradish peroxidase-conjugated
222 anti-mouse, anti-rabbit and anti-rat secondary antibodies for Western blot analysis were
223 obtained from Dianova (Hamburg, Germany), and Alexa Fluor 488 and 555-conjugated
224 secondary antibody for indirect immunofluorescence experiments was purchased from
225 Molecular Probes (Karlsruhe, Germany).

226 **siRNA transfection.** HFF cells were seeded into six-well dishes (2.25×10^5 cells/well) and
227 transfected one day later with 100 pM of either a mix of 4 specific *SPOC1* siRNAs
228 (Dharmacon, Lafayette, CO, USA) or control siRNAs #1 or #3 with Lipofectamine 2000
229 (Invitrogen, Karlsruhe, Germany) using the standard protocol for siRNA transfection
230 provided by the manufacturer.

231 **RNA isolation and quantitative SYBR green real-time PCR (qRT-PCR).** RNA
232 isolation and subsequent quantitative SYBR green qRT-PCR were performed as described
233 elsewhere (29). *SPOC1* transcripts were amplified utilizing the primer pair 5'SPOC1 and
234 3'SPOC1 (Table 1) and normalized against the housekeeping gene *RPL13A* (Ribosomal

235 Protein L13a, primer set contained within the HHK-1 set, Biomol GmbH, Hamburg,
236 Germany).

237 **Multistep growth curve analysis and TaqMan real-time PCR.** Multistep growth curve
238 analyses as well as the quantification of viral DNA in supernatants from infected
239 HFF/control, HFF/SPOC1, and HFF/SPOC (Tet-On) cells were performed as described in
240 a previous study (40).

241 **Chromatin immunoprecipitation (ChIP) assays.** For ChIP assays coupled with qRT-
242 PCR (ChIP-qRT-PCR) HFF cells were infected with TB40/E at an MOI of 0.5 and proteins
243 cross-linked 8 hpi with 1 % formaldehyde for 10 min at room temperature (RT). The
244 reaction was quenched with glycine; cells were washed with PBS and harvested by
245 scraping. After further washing steps chromatin preparation and subsequent ChIP were
246 performed according to “Chromatin preparation” and “Transcription Factor ChIP”
247 protocols obtained from <http://www.blueprint-epigenome.eu/> with slight alterations. In
248 brief, 1.5×10^7 cells were lysed in 1 ml lysis buffer and fragmented to an average length of
249 500-800 bp by sonication using the Bioruptor NextGene UCD 300 (Diagenode SA,
250 Seraing, Belgium). Subsequently, cell debris was cleared by centrifugation and ChIP was
251 performed over night with the fragmented chromatin from 5×10^5 cells, A/G magnetic beads
252 (Merck Chemicals GmbH, Darmstadt, Germany) and α -SPOC1 CR56 antibody or
253 alternatively HA antibody as control in incubation buffer supplemented with protease
254 inhibitors (Sigma-Aldrich, Deisenhofen, Germany) and 0.1 % BSA. After washing the
255 beads with wash buffers I-IV, chromatin was eluted and subjected to proteinase K digestion
256 overnight. Input samples were equally processed in parallel. Finally, chromatin was

257 purified with the QIAquick MinElute PCR Purification Kit (Qiagen, Hilden, Germany) and
258 subjected to SYBRgreen PCR as described elsewhere with primer pairs +788_+732_fw
259 and +788_+732_rev, +39_-46_fw and +39_-46_rev, -1082_-1191_fw and -1082_-
260 1191_rev (29). The average C_t -value was determined from triplicate samples and
261 normalized with standard curves for each primer pair. The identities of the obtained
262 products were confirmed by melting curve analysis.

263 For ChIP-sequencing (ChIP-seq) HFF/SPOC1 (Tet-On) cells were induced with
264 doxycycline (500 ng/ml) one day prior to infection with TB40/E (MOI 0.5). Proteins were
265 cross-linked 8 hpi with 1 % formaldehyde for 10 min at RT followed by quenching of the
266 reaction and several wash steps. Chromatin preparation and subsequent ChIP were
267 performed as described above with some alterations. Thereby, cells were lysed and
268 fragmented to an average length of 200 bp using the Covaris S220 AFA Ultrasonicator.
269 ChIP was performed over night with A/G magnetic beads and α -SPOC1 CR56 antibody in
270 incubation buffer supplemented with protease inhibitors and 0.1 % BSA. In order to obtain
271 the highest DNA yield from 1×10^6 cells, four single ChIPs with each 2.5×10^5 cells were
272 performed, which were pooled after elution as one sample, ultimately resulting in two
273 distinct replicates. ChIP-Seq libraries were generated using the TruSeq ChIP kit (Illumina)
274 and sequenced on an Illumina HiSeq2500 platform. Reads were demultiplexed using
275 Illumina bcl2fastq v2.17.1.14. Fastq files from two flow-cells were then concatenated. A
276 reference genome was created by merging the human reference genome (hsGRCh38v87)
277 and the annotated TB40E_BAC4 HCMV genome (GB: EF999921.1). Alignment to this
278 reference genome was then performed using bowtie2-2.2.9 with standard parameters.

279 Reads were deduplicated with samtools 1.3 and subjected to peak-calling using the MACS2
280 IDR pipeline as outlined in
281 <https://sites.google.com/site/anshulkundaje/projects/idr/deprecated>. For normalized
282 enrichment calculation, data were mean-centered and normalized to input.

283 **Live cell imaging.** HFF/SPOC1 (Tet-On) cells were seeded in live-cell imaging chamber
284 slides (4×10^4 cells/chamber; μ -Slide 8 Well, ibidi GmbH, Planegg, Germany) and 24 h
285 prior to infection SPOC1 overexpression was induced by addition of doxycycline (500
286 ng/ml). In parallel, untreated cells were left as control. SiR-DNA (Spirochrome AG, Stein
287 am Rhein, Germany) was added 2 h prior to infection for tracking of cell nuclei.
288 Subsequently, cells were inoculated with the recombinant reporter virus TB40/E-IE-
289 mNeonGreen at an MOI of 0.05 by centrifugation at 2000 rpm for 10 min at RT.
290 Afterwards, virus supernatants were removed, and cells were supplemented with fresh
291 medium. In order to follow the infection in real time, a Leica TCS SP5 confocal microscope
292 with a complete environmental incubation system was used. Thereby, images of 5 fields
293 per condition were acquired every 15 min for up to 30 hours. The acquired stacks of time
294 series for all fields were automatically analyzed using an ImageJ macro created by B.
295 Kasmapour, Braunschweig, reporting the mean IE signal associated to the cell nuclei in
296 each frame (31).

297 **RESULTS**

298 **SPOC1 is transiently upregulated during HCMV infection**

299 SPOC1 has previously been demonstrated to act as a restriction factor against human
300 adenovirus (HAdV) infection by repressing viral gene expression at the transcriptional
301 level (25). To antagonize this repressive function, HAdV targets SPOC1 for proteasomal
302 degradation immediately upon infection. In order to evaluate the role of SPOC1 during
303 HCMV infection, we inoculated HCMV permissive primary human foreskin fibroblasts
304 (HFF) with the laboratory strain AD169 at a multiplicity of infection (MOI) of 3 and
305 assessed SPOC1 protein levels throughout the HCMV replication cycle (Fig. 1A). In
306 parallel, representatives of the immediate-early (IE), early (E) and late (L) phase of HCMV
307 infection were detected to ensure that the replication cycle has fully proceeded.
308 Interestingly, and in contrast to the HAdV-induced depletion of SPOC1, we observed a
309 transient upregulation of SPOC1 during the early phase of HCMV infection, while at late
310 times post infection SPOC1 levels declined. In order to investigate whether this
311 upregulation is based on increased *SPOC1* transcription, we isolated total RNA at 24 hpi
312 followed by quantitative reverse-transcription PCR (qRT-PCR) (Fig. 1B, left). This
313 revealed only a mild increase of *SPOC1* mRNA (2-fold) when compared to the 6-fold
314 increase in SPOC1 protein abundance (Fig. 1B, right). Consequently, we assume that the
315 upregulation of SPOC1 takes place both on transcript and protein level. Next, we analyzed
316 if the observed upregulation is virus-strain or cell-type dependent. HFFs and retinal
317 pigment epithelial cells (ARPE-19) were infected with the clinical isolate TB40/E and
318 SPOC1 expression levels were analyzed throughout the replication cycle (Fig. 1C and 1D,

319 respectively). In both cases we observed a strong induction of SPOC1 expression
320 culminating at 24 hpi, implying that this event is cell-type and virus-strain independent.
321 Moreover, it appears to be conserved since we also detected increased murine SPOC1
322 levels during MCMV infection beginning at 24 hpi (Fig. 1E). Together, these findings
323 provide evidence that SPOC1 is robustly and specifically upregulated upon CMV infection,
324 raising the question of a pro- or an antiviral function of SPOC1 for viral replication.

325 **Elevated SPOC1 protein levels are induced by an IE or E gene product of HCMV**

326 Next, we set out to investigate whether a viral gene product is responsible for the
327 upregulation of SPOC1 during infection. Since herpesviral gene expression occurs in a
328 cascade fashion with chronological phases termed immediate-early (IE), early (E) and late
329 (L), it is possible to confine the responsible viral protein to a specific expression phase
330 during HCMV infection. First, we assessed whether elevated SPOC1 levels are due to
331 stabilization by an HCMV tegument protein. Therefore, we applied cycloheximide (CHX)
332 in parallel with AD169 infection. This inhibits *de novo* HCMV gene expression but does
333 not affect the abundance of tegument proteins, as confirmed by detection of IE1 and pp65,
334 respectively (Fig. 2A). Western blot analysis at 12 or 24 hpi revealed that SPOC1 is
335 sensitive to CHX treatment (Fig. 2A), while it can be stabilized by MG132 treatment as
336 shown in Figure 2B. These observations are in accordance with literature, where SPOC1
337 was described as a labile protein that is tightly regulated by the proteasome (22). Moreover,
338 no stabilizing effect of tegument proteins was detectable (Fig. 2A, compare lanes 3, 4 and
339 7, 8). As an alternative approach, we used UV-inactivated viral supernatants (UV-AD169)
340 for infection of HFFs in parallel with wild-type AD169 (wt-AD169) and harvested the cells

341 4 and 24 hpi (Fig. 2C). In contrast to AD169-infected HFFs, cells inoculated with UV-
342 inactivated virus did not exhibit increased SPOC1 protein levels. Here, too, IE1 as well as
343 pp65 detection served as a control for UV-inactivation. Consequently, these data
344 demonstrate that *de novo* CMV gene expression is necessary to induce an upregulation of
345 SPOC1. In order to determine if a true late viral protein is the decisive factor, we made use
346 of the viral DNA synthesis inhibitor phosphonoformic acid (PFA). However, incubation of
347 the infected cells with PFA did not abolish SPOC1 upregulation, which was assessed at 72
348 hpi (Fig. 2D). Taken together, these findings indicate that SPOC1 is a labile protein, which
349 is most likely upregulated or stabilized by an IE or E gene product.

350 **IE1 expression induces the upregulation of SPOC1**

351 It has previously been demonstrated that SPOC1 modulates DNA repair kinetics and is
352 recruited to DNA double strand breaks in an ATM-dependent manner (24). Since there is
353 increasing evidence that the IE1 protein is able to modulate the DNA damage response
354 during HCMV infection, we assumed that IE1 might be involved in the upregulation of
355 SPOC1 (41-44). In order to investigate this, we utilized IE1-inducible HFF cells (HFF-IE1
356 Tet-On), and analyzed SPOC1 expression levels in the presence or absence of IE1 (Fig.
357 3A). As evident from Western blot analyses, SPOC1 expression levels were clearly
358 increased in the presence of IE1. In parallel, PML deSUMOylation was detected to monitor
359 the effect of IE1 on cellular proteins. These data demonstrate that IE1 expression alone is
360 sufficient to induce SPOC1 upregulation. We next set out to investigate whether IE1 is
361 required for the increase in SPOC1 levels during HCMV infection. To this end, we infected
362 HFF cells with a high MOI (2) of wild-type AD169 and equivalent genome copy numbers

363 of recombinant HCMV virus strains that either completely lack IE1 (AD169 Δ IE1) or that
364 express the mutant IE1 protein IE1-L174P (AD169/IE1-L174P), which exerts a similar
365 growth defect as the IE1 deletion virus (29). Subsequently, the cells were harvested at
366 different times post infection and subjected to Western blot analysis (Fig. 3B). Intriguingly,
367 SPOC1 upregulation at 24 hpi was attenuated in cells infected with the recombinant virus
368 strains, indicating that functional IE1 is necessary to induce increased SPOC1 protein
369 levels.

370 Since we already demonstrated that SPOC1 is a labile protein that is rapidly
371 degraded by the proteasome (Fig. 2C), we next set out to investigate, if IE1 has a favorable
372 effect on SPOC1 protein stability. Therefore, we assessed SPOC1 protein levels in
373 presence or absence of IE1 while treating the HFF-IE1 Tet-On cells with CHX and
374 harvesting them at different times post treatment (Fig. 3C). While the overall SPOC1
375 expression was increased in presence of IE1, its half-life was not significantly affected
376 (Fig. 3C and D). Taken together, these data allow the assumption that during HCMV
377 infection IE1 is responsible for the observed upregulation of SPOC1 by mechanisms other
378 than protein stabilization.

379 **SPOC1 decrease during HCMV infection takes place in a GSK-3 β -dependent manner**

380 We next set out to investigate the observed decline in SPOC1 abundance at late times of
381 infection in more detail. This decline was particularly prominent in HFF and ARPE-19
382 cells infected with HCMV strain TB40/E (Fig. 1, C and D). Interestingly, Kinkley and
383 colleagues analyzed SPOC1 protein stability in more detail and demonstrated a tight
384 regulation of SPOC1 by the proline-directed serine-threonine kinase GSK-3 β (22). In order

385 to confirm this, we first treated HEK293T and HFF cells with inhibitors of GSK-3 β (LiCl)
386 and the proteasome (MG132) and analyzed SPOC1 expression levels via Western blotting
387 (Fig. 4A). In line with the findings of Kinkley and colleagues, we observed that SPOC1
388 was stabilized upon treatment with either LiCl or MG132, and displayed even stronger
389 signal intensities after treatment with both inhibitors. Intriguingly, analysis of GSK-3 β
390 expression levels throughout the HCMV replicative cycle revealed an increase at late times
391 post infection, which correlated with the decline of SPOC1 abundance (Fig. 4B). Thus, we
392 assumed that GSK-3 β is involved in the decrease of SPOC1 levels at late times post
393 infection. For further investigation, we infected HFFs with HCMV strain TB40/E and
394 applied LiCl at either 1.5 hpi or 48 hpi followed by harvesting at 96 hpi (Fig. 4C).
395 Regardless of when the inhibitor was added, the decrease of SPOC1 levels was efficiently
396 blocked, even if LiCl was added at late times post infection and MCP levels remained
397 equal. Since the decline of SPOC1 was even more prominent in infected ARPE-19 cells
398 (Fig. 1D), we next added LiCl and two additional GSK-3 β inhibitors (SB-216763,
399 CHIR99021) at 48 hpi and harvested ARPE-19 cells 4 days post infection with HCMV
400 strain TB40/E (Fig. 4D). In line with our previous findings, we observed a block of SPOC1
401 decline with LiCl as well as CHIR99021. However, SB-216763 had no stabilizing effect
402 on SPOC1. Taken together, our data suggest that the observed decrease in SPOC1 levels
403 during the late stage of HCMV infection is in part mediated by GSK-3 β .

404 **SPOC1 overexpression inhibits the onset of viral IE gene expression**

405 Next, we wanted to address the relevance of SPOC1 for lytic HCMV replication. First, we
406 generated cells that stably overexpress SPOC1 which was accomplished by lentiviral

407 transduction of primary HFFs using a vector encoding for *SPOC1*. In parallel, the cloning
408 vector served to generate control cells. Subsequent geneticin selection resulted in cell
409 populations termed HFF/SPOC1 and HFF/control, respectively. These cells were then
410 characterized by Western blot analysis, which revealed successful SPOC1 overexpression
411 in the HFF/SPOC1 cells (Fig. 5A) concurrent with a high transduction efficiency of almost
412 100% as assessed by indirect immunofluorescence detection (Fig. 5B). In order to analyze
413 the impact of SPOC1 overexpression on HCMV replication, the generated cells were
414 infected with the HCMV laboratory strain AD169 at an MOI of 1, harvested at different
415 time points of the replication cycle and expression kinetics of viral immediate early, early,
416 and late proteins were assessed by Western blotting (Fig. 6A). The SPOC1 overexpressing
417 cells showed decreased viral early and late protein expression when compared to control
418 cells which was most prominent for pUL97 and pp71 as revealed by quantification of the
419 Western blot signals (Fig. 6B).

420 Since cellular restriction is saturable and effects might be masked at high MOI, we next
421 applied multistep growth curve analyses at low-multiplicity of infection. We infected cells
422 with three different MOIs (0.005, 0.001, 0.0005) and harvested virus-containing cell
423 supernatants at indicated times post infection (Fig. 6C). Subsequently, the supernatants
424 were subjected to quantitative real-time PCR to determine the HCMV genome equivalents.
425 As evident from Figure 6C, SPOC1 overexpression strongly impaired virus growth under
426 low MOI conditions and caused an up to 3 log₁₀ reduction in viral progeny release. SPOC1
427 did not affect virus uptake and/or genome delivery into the nucleus since quantification of
428 intranuclear viral genomes did not reveal a significant difference between control and
429 SPOC1 overexpressing cells (Fig. 6D) In order to test if SPOC1 overexpression already

430 acts on the initiation of viral gene expression, HFF/SPOC1 and HFF/control cells were
431 infected in parallel with 100 IE1 forming units (IEU) of HCMV strains AD169 or TB40/E.
432 24 hours later, the cells were stained for IE1 to determine the number of cells exhibiting an
433 initiation of IE gene expression. Intriguingly, we detected a four-fold reduction in IE1-
434 positive cells when SPOC1 was overexpressed and infected with the laboratory strain
435 AD169 (Fig. 6E, left). An even more pronounced effect was observed after inoculation
436 with the clinical strain TB40/E (Fig. 6E, right). Taken together, our data demonstrate that
437 overexpression of SPOC1 negatively affects virus growth, which could be attributed to a
438 restriction of IE gene expression. This finding, in line with the observed MOI-dependency,
439 strongly suggests that SPOC1 acts as a cellular restriction factor for cytomegalovirus
440 infection.

441 **SPOC1 overexpression during the first hours of HCMV infection is critical for**
442 **efficient restriction**

443 In order to analyze if high SPOC1 levels prior to infection are necessary for an efficient
444 HCMV restriction, we generated HFF cells that were able to induce SPOC1 overexpression
445 upon treatment with doxycycline. In order to accomplish this, we made use of the Lenti-X
446 Tet-On Advanced Inducible Expression System (Clontech, Palo Alto, CA, USA). After
447 insertion of the coding sequence for Flag-tagged SPOC1 into the pLVX Tet-On Advanced
448 vector, lentiviral transduction of HFF cells and selection with puromycin and geneticin
449 yielded a cell population termed HFF/SPOC1 (Tet-On). These cells showed a strong
450 inducibility already 8 hours post treatment with doxycycline (Fig. 7, A and B). First, we
451 wanted to know whether high SPOC1 levels are able to restrict the onset of immediate-

452 early RNA expression. Thus, cells were either treated with doxycycline for 24 h (+Dox) or
453 not treated (-Dox), subsequently infected with HCMV strain AD169 (MOI 0.001) and total
454 RNA was isolated at 8 hpi. Quantification of IE1 transcripts revealed a strong reduction of
455 IE1 mRNA levels upon overexpression of SPOC1 (Fig. 7C). Next, we induced SPOC1
456 overexpression either 24 hours prior, in parallel or 8 hours post infection with 100 IEU of
457 AD169 and counted IE1-positive cells 24 hours post infection (Fig. 7D). Interestingly, we
458 found that restriction of the initiation of IE gene expression was most effective when
459 SPOC1 was pre-expressed in the infected cells, leading to an 8-fold decrease in IE-positive
460 cells (Fig. 7D). A significant restriction was still observed when SPOC1 overexpression
461 was induced in parallel with the infection, whereas its induction at 8 hpi no longer affected
462 the onset of IE gene expression. Consistent with these results, viral progeny release was
463 inhibited up to 3 logs₁₀ when SPOC1 overexpression was induced prior to infection
464 (Fig. 7E). From these findings we conclude that high SPOC1 protein levels prior to the
465 initiation of viral IE gene expression efficiently restrict HCMV replication.

466 To further elucidate whether SPOC1 overexpression delays or completely
467 abrogates the onset of viral IE gene expression, we tracked the kinetics of HCMV gene
468 expression in real time using live-cell imaging. HFF/SPOC1 (Tet-On) cells were induced
469 with doxycycline 24 h prior to infection, while untreated cells were used in parallel as a
470 control. For real time monitoring we made use of the recombinant reporter virus TB40/E-
471 IE-mNeonGreen, which has previously been used by Kasmapour and colleagues to monitor
472 IE protein expression kinetics (31). The dynamics of early viral gene expression (up to 30
473 hpi) were investigated after infection at an MOI of 0.05 followed by automated whole
474 frame evaluation and quantification with ImageJ-based software (Fig. 8A). The generated

475 data set provided us with two different pieces of information. On the one hand, detection
476 of the onset of viral IE gene expression was possible, which is characterized by a drop in
477 mean signal intensity due to the increased area of a true signal compared to auto-
478 fluorescence. On the other hand, the rate of gene expression could be assessed by
479 measuring the steepness of the slope. The main conclusions were that SPOC1
480 overexpression appeared to delay the onset of viral IE gene expression and also to suppress
481 gene expression. Within the control cells, first IE reporter signals were detected between 5
482 to 10 hpi (Fig. 8B) and steadily increased with proceeding infection (Fig. 8A). In contrast,
483 SPOC1 overexpression significantly delayed the onset of IE gene expression, starting
484 between 9 to 15 hpi (Fig. 8B), and showed a reduced increase (Fig. 8A). However, the
485 automated whole frame evaluation and quantification is confined to reporter signal
486 positivity, thus ignoring infected cells that lack *de novo* viral gene expression. When
487 comparing images from infected cells +/- doxycycline treatment, it becomes clear that a
488 significantly lower number of cells expressed IE-mNeonGreen upon overexpression of
489 SPOC1 (Fig. 8C). To further analyze the heterogeneity of cells exhibiting viral gene
490 expression we performed manual single cell tracking. Using this, we assessed the time of
491 onset and the maximal rate of IE gene expression for up to 20 individual HCMV-infected
492 cells (Fig. 8D and E, respectively). Within induced and non-induced cells, we observed a
493 high variability regarding the start of *de novo* viral gene expression ranging from 4.5 to
494 20 hpi (Fig. 8D). Although a slight tendency towards a SPOC1-mediated inhibition was
495 apparent, the overall values revealed no significant difference in the maximal rate of viral
496 gene expression in SPOC1-positive cells (Fig. 8E). However, single-cell tracking is
497 confined to reporter signal positivity, thus ignoring infected cells that lack *de novo* viral

498 gene expression, which were taken into the consideration by the whole-frame analysis. In
499 summary, this strongly argues for a scenario whereby high SPOC1 levels are able to induce
500 a complete silencing of viral IE gene expression.

501 **Depletion of endogenous SPOC1 augments the initiation of IE gene expression**

502 Overall these findings argue for an antiviral function of SPOC1 when it is present at high
503 levels in HFF cells. In order to investigate whether endogenous SPOC1 is sufficient for
504 restriction of HCMV, we used two different approaches to deplete SPOC1 from primary
505 HFF cells. On the one hand we applied siRNA mediated knockdown by transiently
506 transfecting a mix of siRNAs directed against SPOC1. On the other hand we used the
507 CRISPR/Cas9 technology to establish stable SPOC1 knockout HFFs. In order to
508 accomplish this, we designed a specific guide RNA (gRNA) directed against SPOC1,
509 cloned it into the CRISPRv2 lentiviral plasmid followed by lentiviral transduction of HFF
510 cells (28). Puromycin selection yielded HFF/SPOC1-k.o. cell as well as control cell
511 populations, termed HFF/CRISPRv2, which were generated with the empty vector
512 CRISPRv2. For both methods, efficient SPOC1 depletion was verified by Western blot
513 analysis (Fig. 9A and B). Next, SPOC1-depleted HFFs (HFF+siSPOC1 or HFF/SPOC1-
514 k.o.) in parallel with the respective control cells were infected with HCMV (100 IEU/well)
515 followed by immunostaining of IE1 at 24 hpi. Intriguingly, we observed a significant
516 increase of IE1-positive cells in the SPOC1 knockout and knockdown cells compared to
517 the respective control cells, demonstrating that endogenous SPOC1 contributes to a
518 repression of viral IE gene expression (Fig. 9C and D). IE1 mRNA was also increased in
519 SPOC1 knockout cells when infection was performed at a MOI of 0.01 (Fig. 9E). In

520 contrast, SPOC1 depletion exerted no significant effect under conditions of high MOI
521 infection (Fig. 9F). Finally, multistep growth curve analyses confirmed the inhibitory effect
522 of SPOC1 on HCMV replication (Fig. 9G, left panel). This was even more pronounced
523 when viruses exhibiting a deletion in the regions encoding the ND10 antagonistic proteins
524 IE1 (AD169/del-IE1) or pp71 (AD169/del-pp71) were used in this analyses (Fig. 9G,
525 middle and right panel).

526 **SPOC1 specifically associates with the proximal enhancer region of the major**
527 **immediate-early promoter**

528 Initiation of HCMV IE gene expression is driven by the major immediate-early promoter
529 (MIEP). Since SPOC1 is able to directly interact with DNA, a possible mode of action
530 could be a binding of SPOC1 to the MIEP followed by a subsequent epigenetic modulation.
531 In order to address this question, we performed SPOC1-specific chromatin
532 immunoprecipitation (ChIP) in parallel with a negative control (HA) and investigated
533 different regions of the CMV promoter by qPCR (Fig. 10A) (23). While SPOC1 showed
534 no significant enrichment over the control antibody HA (Fig. 10A) within regions outside
535 the CMV enhancer (ranges of +788 to +732 and -1082 to -1191 relative to the MIEP start
536 site), we found specific enrichment of SPOC1 within the proximal enhancer region of the
537 MIEP. In order to gain more insight into the binding profile of SPOC1, we performed ChIP
538 coupled with deep sequencing (ChIP-seq) analyses on material isolated from HFF/SPOC1
539 (Tet-On) cells induced with doxycycline 24 h prior to infection with TB40/E at an MOI of
540 0.5 and performed cross-linking at 8 hpi. After quality control and alignment against the
541 reference genome, generated by merging the human reference genome (hsGRCh38v87)

542 with the annotated TB40E_BAC4 HCMV genome (GB: EF999921.1), we utilized the
543 MACS2 IDR pipeline for peak-calling in both generated replicates. We had total numbers
544 of 39 and 51 million reads for replicates 1 and 2, while 0.2 % and 0.17 % of them mapped
545 to the TB40/E genome, respectively. Among these, the majority (83 %) mapped within the
546 region of 207.200 to 208.300 bp of the HCMV genome showing a more than 500-fold
547 enrichment (Fig. 10B). Intriguingly, this region corresponded to the site where the MIEP
548 is located within the HCMV genome (Fig. 10C). Therefore, we conclude that SPOC1
549 targets the viral genome upon HCMV infection and binds within the CMV
550 enhancer/promoter region, thereby mediating a restriction of viral IE gene expression.

551 **DISCUSSION**

552 In this report, we investigated the role of the cellular protein SPOC1 as a putative restriction
553 factor against HCMV infection. Previous studies reported an antiviral activity of SPOC1
554 during human adenovirus infection as well as during HIV-1 replication (25, 26). Both
555 studies demonstrated that SPOC1 levels rapidly diminish early upon virus infection.
556 Interestingly and in contrast to HAdV and HIV-1, we identified that SPOC1 is robustly and
557 specifically upregulated by HCMV infection (Fig. 1A). This upregulation appears to be
558 conserved between different HCMV strains and MCMV and could be observed upon
559 infection of various cell types (Fig. 1C - E). SPOC1 has previously been described to act
560 as a modulator of DNA double strand break repair (24). Intriguingly, HCMV differs from
561 HAdV in its requirement for an active DNA damage response (DDR). While HAdV has
562 evolved mechanisms to efficiently inhibit the cellular DDR, HCMV stimulates components
563 of the DDR machinery during the course of its replicative cycle. In particular, the master
564 regulator ATM was demonstrated to be required for efficient HCMV replication (43).
565 Thus, we hypothesize that SPOC1 may undergo upregulation as a component of the virus-
566 induced DDR while it is rapidly degraded after HAd5C5 infection as a mechanism of AdV-
567 mediated DDR countermeasures. Furthermore, we were able to attribute the increase in
568 SPOC1 abundance to IE1 expression (Fig. 3A and B). Intriguingly, Kulkarni and Fortunato
569 reported that homologous recombination (HR) as one branch of the DNA double strand
570 break repair is increased upon HCMV infection which was demonstrated to be specifically
571 stimulated by IE1 expression (41). In line with this, SPOC1 was found to modulate DNA
572 repair kinetics by shifting the balance between non-homologous end joining (NHEJ) and
573 HR, the latter being favored (24). After initial activation of the DDR during the early phase,

574 HCMV inhibits the DDR by protein mislocalization during late stages of infection (45).
575 Hence, the decline of SPOC1 levels that we observed during our studies may correlate with
576 an overall inactivation of the cellular DDR during the late phase of replication. Moreover,
577 we were able to demonstrate that the drop of SPOC1 abundance is GSK-3 β dependent.
578 This fits with recent observations demonstrating that SPOC1 degradation during HIV-1
579 infection also occurs in a GSK-3 β -dependent manner (26). However, whereas during HIV-
580 1 infection the accessory protein Vpr was identified as the responsible viral factor, the
581 HCMV regulatory proteins inducing SPOC1 downregulation remain to be determined.
582 Since a priming phosphorylation of SPOC1 is a prerequisite for subsequent
583 phosphorylation by GSK-3 β , a possible candidate factor might be the viral protein kinase
584 pUL97 which will be investigated in future studies (46).

585 In order to elucidate the role of SPOC1 for HCMV replication we generated
586 primary human fibroblasts overexpressing SPOC1 and found that high protein levels
587 significantly reduced virus growth (Fig. 6C). In line with this, SPOC1 depletion led to
588 enhanced HCMV infectivity (Fig. 9C and D). We demonstrate that SPOC1 interferes with
589 the initiation of viral IE gene expression and this occurs in a MOI-dependent manner. MOI-
590 dependency is a hallmark of many restriction factors (2, 47, 48). This is due to limiting
591 amounts of pre-existing host factors that may either be saturated by incoming viral
592 genomes or antagonized by viral factors. Furthermore, using inducible expression systems
593 we were able to narrow down the time point of SPOC1 action to very early events of the
594 viral replication cycle: when high SPOC1 levels were present at the time point of HCMV
595 infection, efficient restriction was observed while a later SPOC1 upregulation had no
596 significant effects (Fig. 7D). Moreover, results obtained by live cell imaging experiments

597 suggest that SPOC1 affects IE gene expression not only by delaying its onset and reducing
598 its rate (Fig. 8A and B), but by completely abrogating the initiation of viral gene expression
599 (Fig. 8C). Thus, we speculate that high SPOC1 levels constitute an obstacle for the virus
600 that cannot be overcome, leading to a complete shutdown of viral IE gene expression.

601 Our findings corroborate previous studies by Schreiner and colleagues as well as
602 Hofmann and colleagues which described SPOC1 as an antiviral restriction factor targeting
603 HAdV and in part HIV-1. While during HIV-1 infection SPOC1 appears to play a dual role
604 by promoting HIV-1 integration and by repressing viral gene expression, an exclusively
605 repressive role has been described for HAdV infection (25). The group demonstrated that
606 SPOC1 represses HAdV promoter activity and suggested that it targets incoming HAdV
607 genomes immediately upon infection. On the contrary, Komatsu and colleagues were not
608 able to confirm this hypothesis by live cell imaging techniques. They rather suggested that
609 SPOC1 affects replicating or replicated viral genomes during the late stage of infection
610 (49). Thus, the exact mechanism how SPOC1 is able to affect viral gene expression
611 requires further investigation.

612 Interestingly, we observed by ChIPseq experiments that SPOC1 exclusively
613 associates with a specific gene region of HCMV, namely the proximal enhancer region of
614 the MIEP (Fig. 10). This regulatory element exerts a critical role for HCMV and there is
615 increasing evidence that epigenetic modifications of the chromatin structure around the
616 MIEP control the onset of viral gene expression (50, 51). So far, it is not clear whether
617 SPOC1 associates with viral DNA directly or in an indirect manner, for instance via
618 interaction with H3K4me2/3. Intriguingly, SPOC1 was described to interact with several
619 key regulators of chromatin structure, e.g. the transcriptional co-repressor KAP1 and

620 several lysine methyltransferases (KMTs) such as SETDB1, GLP, and G9A (23, 24).
621 Consequently, we hypothesize that SPOC1 may serve as a recruitment factor for these
622 heterochromatin building proteins which may then establish a repressive chromatin
623 structure leading to a shutdown of viral IE gene expression. A promising candidate would
624 be the co-repressor protein KAP1, which was recently proposed to act as a critical factor
625 regulating the release of HCMV from latency by a phosphorylation switch (52). In addition,
626 several studies demonstrated that in non-permissive cells the MIEP is associated with a
627 number of other heterochromatin building factors such as the KMTs Suvar(3-9)H1,
628 SETDB1, and G9A (51, 53-55). Since SPOC1 binds to several of the aforementioned
629 heterochromatin proteins, we strongly assume that its restrictive function is exerted by
630 recruitment of at least one of them. Whether these factors act as one large repressor
631 complex or are recruited in a sequential manner needs to be clarified by future studies.
632 Furthermore, since there is a considerable variation of expression levels between cell types,
633 we assume that restriction by SPOC1 occurs in a cell-type dependent manner. Highest
634 SPOC1 transcript levels were described in testis, more precisely in spermatogonia (21).
635 Therefore, one may speculate that SPOC1 contributes to the intrinsic defense of male germ
636 cells against HCMV infection. In summary, our study adds a novel factor to the host cell
637 endowment contributing to intrinsic immunity against cytomegalovirus infections.

638 **ACKNOWLEDGEMENT**

639 We thank M. Mach (Erlangen, Germany), M. Marschall (Erlangen, Germany), A. Ensser
640 (Erlangen, Germany), B. Plachter (Mainz, Germany), and W. Britt (Birmingham, USA) for
641 providing valuable reagents for this study. This work was supported by the Deutsche
642 Forschungsgemeinschaft (SFB796, TP B3 and STA357/7-1 to TS; SFB900 TP B2 to LC-
643 S), the Interdisciplinary Center for Clinical Research Erlangen (IZKF Erlangen, project
644 A71 to TS) and the Wilhelm Sander Stiftung (2016.087.1 to TS).

645 REFERENCES

- 646 1. **Hatzioannou T, Bieniasz PD.** 2011. Antiretroviral restriction factors. *Curr Opin*
647 *Virol* **1**:526-532.
- 648 2. **Tavalai N, Papior P, Rechter S, Leis M, Stamminger T.** 2006. Evidence for a
649 role of the cellular ND10 protein PML in mediating intrinsic immunity against
650 human cytomegalovirus infections. *J Virol* **80**:8006-8018.
- 651 3. **Gariano GR, Dell'Oste V, Bronzini M, Gatti D, Luganini A, De Andrea M,**
652 **Gribaudo G, Gariglio M, Landolfo S.** 2012. The intracellular DNA sensor IFI16
653 gene acts as restriction factor for human cytomegalovirus replication. *PLoS Pathog*
654 **8**:e1002498.
- 655 4. **Korioth F, Maul GG, Plachter B, Stamminger T, Frey J.** 1996. The nuclear
656 domain 10 (ND10) is disrupted by the human cytomegalovirus gene product IE1.
657 *Exp Cell Res* **229**:155-158.
- 658 5. **Tavalai N, Kraiger M, Kaiser N, Stamminger T.** 2008. Insertion of an EYFP-
659 pp71 (UL82) coding sequence into the human cytomegalovirus genome results in
660 a recombinant virus with enhanced viral growth. *J Virol* **82**:10543-10555.
- 661 6. **Adler M, Tavalai N, Muller R, Stamminger T.** 2011. Human cytomegalovirus
662 immediate-early gene expression is restricted by the nuclear domain 10 component
663 Sp100. *J Gen Virol* **92**:1532-1538.
- 664 7. **Everett RD, Chelbi-Alix MK.** 2007. PML and PML nuclear bodies: implications
665 in antiviral defence. *Biochimie* **89**:819-830.
- 666 8. **Glass M, Everett RD.** 2013. Components of promyelocytic leukemia nuclear
667 bodies (ND10) act cooperatively to repress herpesvirus infection. *J Virol* **87**:2174-
668 2185.
- 669 9. **Woodhall DL, Groves IJ, Reeves MB, Wilkinson G, Sinclair JH.** 2006. Human
670 Daxx-mediated repression of human cytomegalovirus gene expression correlates
671 with a repressive chromatin structure around the major immediate early promoter.
672 *J Biol Chem* **281**:37652-37660.
- 673 10. **Saffert RT, Kalejta RF.** 2006. Inactivating a cellular intrinsic immune defense
674 mediated by Daxx is the mechanism through which the human cytomegalovirus
675 pp71 protein stimulates viral immediate-early gene expression. *J Virol* **80**:3863-
676 3871.
- 677 11. **Lukashchuk V, McFarlane S, Everett RD, Preston CM.** 2008. Human
678 cytomegalovirus protein pp71 displaces the chromatin-associated factor ATRX
679 from nuclear domain 10 at early stages of infection. *J Virol* **82**:12543-12554.
- 680 12. **Kim YE, Lee JH, Kim ET, Shin HJ, Gu SY, Seol HS, Ling PD, Lee CH, Ahn**
681 **JH.** 2011. Human cytomegalovirus infection causes degradation of Sp100 proteins
682 that suppress viral gene expression. *J Virol* **85**:11928-11937.
- 683 13. **Cantrell SR, Bresnahan WA.** 2005. Interaction between the human
684 cytomegalovirus UL82 gene product (pp71) and hDaxx regulates immediate-early
685 gene expression and viral replication. *J Virol* **79**:7792-7802.
- 686 14. **Gawn JM, Greaves RF.** 2002. Absence of IE1 p72 protein function during low-
687 multiplicity infection by human cytomegalovirus results in a broad block to viral
688 delayed-early gene expression. *J Virol* **76**:4441-4455.

- 689 15. **Dell'Oste V, Gatti D, Gugliesi F, De Andrea M, Bawadekar M, Lo Cigno I,**
690 **Biolatti M, Vallino M, Marschall M, Gariglio M, Landolfo S.** 2014. Innate
691 nuclear sensor IFI16 translocates into the cytoplasm during the early stage of in
692 vitro human cytomegalovirus infection and is entrapped in the egressing virions
693 during the late stage. *J Virol* **88**:6970-6982.
- 694 16. **Biolatti M, Dell'Oste V, Pautasso S, von Einem J, Marschall M, Plachter B,**
695 **Gariglio M, De Andrea M, Landolfo S.** 2016. Regulatory Interaction between the
696 Cellular Restriction Factor IFI16 and Viral pp65 (pUL83) Modulates Viral Gene
697 Expression and IFI16 Protein Stability. *J Virol* **90**:8238-8250.
- 698 17. **Ahn JH, Hayward GS.** 1997. The major immediate-early proteins IE1 and IE2 of
699 human cytomegalovirus colocalize with and disrupt PML-associated nuclear bodies
700 at very early times in infected permissive cells. *J Virol* **71**:4599-4613.
- 701 18. **Ahn JH, Hayward GS.** 2000. Disruption of PML-associated nuclear bodies by IE1
702 correlates with efficient early stages of viral gene expression and DNA replication
703 in human cytomegalovirus infection. *Virology* **274**:39-55.
- 704 19. **Kelly C, Van Driel R, Wilkinson GW.** 1995. Disruption of PML-associated
705 nuclear bodies during human cytomegalovirus infection. *J Gen Virol* **76** (Pt
706 **11**):2887-2893.
- 707 20. **Mohrmann G, Hengstler JG, Hofmann TG, Endeke SU, Lee B, Stelzer C, Zabel**
708 **B, Brieger J, Hasenclever D, Tanner B, Sagemueller J, Shouli J, Will H,**
709 **Winterpacht A.** 2005. SPOC1, a novel PHD-finger protein: association with
710 residual disease and survival in ovarian cancer. *Int J Cancer* **116**:547-554.
- 711 21. **Bordlein A, Scherthan H, Nelkenbrecher C, Molter T, Bosl MR, Dippold C,**
712 **Birke K, Kinkley S, Staeger H, Will H, Winterpacht A.** 2011. SPOC1 (PHF13)
713 is required for spermatogonial stem cell differentiation and sustained
714 spermatogenesis. *J Cell Sci* **124**:3137-3148.
- 715 22. **Kinkley S, Staeger H, Mohrmann G, Rohaly G, Schaub T, Kremmer E,**
716 **Winterpacht A, Will H.** 2009. SPOC1: a novel PHD-containing protein
717 modulating chromatin structure and mitotic chromosome condensation. *J Cell Sci*
718 **122**:2946-2956.
- 719 23. **Chung HR, Xu C, Fuchs A, Mund A, Lange M, Staeger H, Schubert T, Bian C,**
720 **Dunkel I, Eberharter A, Regnard C, Klinker H, Meierhofer D, Cozzuto L,**
721 **Winterpacht A, Di Croce L, Min J, Will H, Kinkley S.** 2016. PHF13 is a
722 molecular reader and transcriptional co-regulator of H3K4me2/3. *Elife* **5**.
- 723 24. **Mund A, Schubert T, Staeger H, Kinkley S, Reumann K, Kriegs M, Fritsch L,**
724 **Battisti V, Ait-Si-Ali S, Hoffbeck AS, Soutoglou E, Will H.** 2012. SPOC1
725 modulates DNA repair by regulating key determinants of chromatin compaction
726 and DNA damage response. *Nucleic Acids Res* **40**:11363-11379.
- 727 25. **Schreiner S, Kinkley S, Burck C, Mund A, Wimmer P, Schubert T, Groitl P,**
728 **Will H, Dobner T.** 2013. SPOC1-mediated antiviral host cell response is
729 antagonized early in human adenovirus type 5 infection. *PLoS Pathog* **9**:e1003775.
- 730 26. **Hofmann S, Dehn S, Businger R, Bolduan S, Schneider M, Debyser Z, Brack-**
731 **Werner R, Schindler M.** 2017. Dual role of the chromatin-binding factor PHF13
732 in the pre- and post-integration phases of HIV-1 replication. *Open Biol* **7**.

- 733 27. **Schilling EM, Scherer M, Reuter N, Schweininger J, Muller YA, Stamminger**
734 **T.** 2017. The Human Cytomegalovirus IE1 Protein Antagonizes PML Nuclear
735 Body-Mediated Intrinsic Immunity via the Inhibition of PML De Novo
736 SUMOylation. *J Virol* **91**.
- 737 28. **Sanjana NE, Shalem O, Zhang F.** 2014. Improved vectors and genome-wide
738 libraries for CRISPR screening. *Nat Methods* **11**:783-784.
- 739 29. **Scherer M, Otto V, Stump JD, Klingl S, Muller R, Reuter N, Muller YA, Sticht**
740 **H, Stamminger T.** 2015. Characterization of Recombinant Human
741 Cytomegaloviruses Encoding IE1 Mutants L174P and 1-382 Reveals that Viral
742 Targeting of PML Bodies Perturbs both Intrinsic and Innate Immune Responses. *J*
743 *Virol* **90**:1190-1205.
- 744 30. **Sinzger C, Hahn G, Digel M, Katona R, Sampaio KL, Messerle M, Hengel H,**
745 **Koszinowski U, Brune W, Adler B.** 2008. Cloning and sequencing of a highly
746 productive, endotheliotropic virus strain derived from human cytomegalovirus
747 TB40/E. *J Gen Virol* **89**:359-368.
- 748 31. **Kasmapour B, Kubsch T, Rand U, Eiz-Vesper B, Messerle M, Vondran FWR,**
749 **Wiegmann B, Haverich A, Cicin-Sain L.** 2018. Myeloid Dendritic Cells Repress
750 Human Cytomegalovirus Gene Expression and Spread by Releasing Interferon-
751 Unrelated Soluble Antiviral Factors. *J Virol* **92**.
- 752 32. **Bootz A, Karbach A, Spindler J, Kropff B, Reuter N, Sticht H, Winkler TH,**
753 **Britt WJ, Mach M.** 2017. Protective capacity of neutralizing and non-neutralizing
754 antibodies against glycoprotein B of cytomegalovirus. *PLoS Pathog* **13**:e1006601.
- 755 33. **Hofmann H, Floss S, Stamminger T.** 2000. Covalent modification of the
756 transactivator protein IE2-p86 of human cytomegalovirus by conjugation to the
757 ubiquitin-homologous proteins SUMO-1 and hSMT3b. *J Virol* **74**:2510-2524.
- 758 34. **Scherer M, Klingl S, Sevana M, Otto V, Schilling EM, Stump JD, Muller R,**
759 **Reuter N, Sticht H, Muller YA, Stamminger T.** 2014. Crystal structure of
760 cytomegalovirus IE1 protein reveals targeting of TRIM family member PML via
761 coiled-coil interactions. *PLoS Pathog* **10**:e1004512.
- 762 35. **Winkler M, Rice SA, Stamminger T.** 1994. UL69 of human cytomegalovirus, an
763 open reading frame with homology to ICP27 of herpes simplex virus, encodes a
764 transactivator of gene expression. *J Virol* **68**:3943-3954.
- 765 36. **Andreoni M, Faircloth M, Vugler L, Britt WJ.** 1989. A rapid microneutralization
766 assay for the measurement of neutralizing antibody reactive with human
767 cytomegalovirus. *J Virol Methods* **23**:157-167.
- 768 37. **Sanchez V, Sztul E, Britt WJ.** 2000. Human cytomegalovirus pp28 (UL99)
769 localizes to a cytoplasmic compartment which overlaps the endoplasmic reticulum-
770 golgi-intermediate compartment. *J Virol* **74**:3842-3851.
- 771 38. **Waldo FB, Britt WJ, Tomana M, Julian BA, Mestecky J.** 1989. Non-specific
772 mesangial staining with antibodies against cytomegalovirus in immunoglobulin-A
773 nephropathy. *Lancet* **1**:129-131.
- 774 39. **Gebert S, Schmolke S, Sorg G, Floss S, Plachter B, Stamminger T.** 1997. The
775 UL84 protein of human cytomegalovirus acts as a transdominant inhibitor of
776 immediate-early-mediated transactivation that is able to prevent viral replication. *J*
777 *Virol* **71**:7048-7060.

- 778 40. **Lorz K, Hofmann H, Berndt A, Tavalai N, Mueller R, Schlotzer-Schrehardt**
779 **U, Stamminger T.** 2006. Deletion of open reading frame UL26 from the human
780 cytomegalovirus genome results in reduced viral growth, which involves impaired
781 stability of viral particles. *J Virol* **80**:5423-5434.
- 782 41. **Kulkarni AS, Fortunato EA.** 2011. Stimulation of homology-directed repair at I-
783 SceI-induced DNA breaks during the permissive life cycle of human
784 cytomegalovirus. *J Virol* **85**:6049-6054.
- 785 42. **Castillo JP, Frame FM, Rogoff HA, Pickering MT, Yurochko AD, Kowalik**
786 **TF.** 2005. Human cytomegalovirus IE1-72 activates ataxia telangiectasia mutated
787 kinase and a p53/p21-mediated growth arrest response. *J Virol* **79**:11467-11475.
- 788 43. **E X, Pickering MT, Debatis M, Castillo J, Lagadinos A, Wang S, Lu S,**
789 **Kowalik TF.** 2011. An E2F1-mediated DNA damage response contributes to the
790 replication of human cytomegalovirus. *PLoS Pathog* **7**:e1001342.
- 791 44. **Kulkarni AS, Fortunato EA.** 2014. Modulation of homology-directed repair in
792 T98G glioblastoma cells due to interactions between wildtype p53, Rad51 and
793 HCMV IE1-72. *Viruses* **6**:968-985.
- 794 45. **Gaspar M, Shenk T.** 2006. Human cytomegalovirus inhibits a DNA damage
795 response by mislocalizing checkpoint proteins. *Proc Natl Acad Sci U S A*
796 **103**:2821-2826.
- 797 46. **Fiol CJ, Mahrenholz AM, Wang Y, Roeske RW, Roach PJ.** 1987. Formation of
798 protein kinase recognition sites by covalent modification of the substrate.
799 Molecular mechanism for the synergistic action of casein kinase II and glycogen
800 synthase kinase 3. *J Biol Chem* **262**:14042-14048.
- 801 47. **Tavalai N, Stamminger T.** 2011. Intrinsic cellular defense mechanisms targeting
802 human cytomegalovirus. *Virus Res* **157**:128-133.
- 803 48. **Wagenknecht N, Reuter N, Scherer M, Reichel A, Muller R, Stamminger T.**
804 2015. Contribution of the Major ND10 Proteins PML, hDaxx and Sp100 to the
805 Regulation of Human Cytomegalovirus Latency and Lytic Replication in the
806 Monocytic Cell Line THP-1. *Viruses* **7**:2884-2907.
- 807 49. **Komatsu T, Will H, Nagata K, Wodrich H.** 2016. Imaging analysis of nuclear
808 antiviral factors through direct detection of incoming adenovirus genome
809 complexes. *Biochem Biophys Res Commun* **473**:200-205.
- 810 50. **Nevels M, Nitzsche A, Paulus C.** 2011. How to control an infectious bead string:
811 nucleosome-based regulation and targeting of herpesvirus chromatin. *Rev Med*
812 *Virol* **21**:154-180.
- 813 51. **Reeves MB.** 2011. Chromatin-mediated regulation of cytomegalovirus gene
814 expression. *Virus Res* **157**:134-143.
- 815 52. **Rauwel B, Jang SM, Cassano M, Kapopoulou A, Barde I, Trono D.** 2015.
816 Release of human cytomegalovirus from latency by a KAP1/TRIM28
817 phosphorylation switch. *Elife* **4**.
- 818 53. **Murphy JC, Fischle W, Verdin E, Sinclair JH.** 2002. Control of cytomegalovirus
819 lytic gene expression by histone acetylation. *EMBO J* **21**:1112-1120.
- 820 54. **Reeves MB, Sinclair JH.** 2010. Analysis of latent viral gene expression in natural
821 and experimental latency models of human cytomegalovirus and its correlation
822 with histone modifications at a latent promoter. *J Gen Virol* **91**:599-604.

- 823 55. **Groves IJ, Reeves MB, Sinclair JH.** 2009. Lytic infection of permissive cells with
824 human cytomegalovirus is regulated by an intrinsic 'pre-immediate-early'
825 repression of viral gene expression mediated by histone post-translational
826 modification. *J Gen Virol* **90**:2364-2374.
827

828 **FIGURE LEGENDS**

829 **Figure 1. SPOC1 is transiently upregulated during HCMV infection.**

830 (A) HFF cells were infected with HCMV laboratory strain AD169 at an MOI of 3 and
831 harvested at the indicated time points post infection. Total-cell extracts were prepared,
832 separated by SDS-PAGE and subjected to immunoblotting with mouse monoclonal
833 antibody p63-27 (IE1), BS 510 (UL44), 28-4 (MCP), and rat monoclonal SPOC1 antibody.
834 (B) HFF cells were infected with HCMV laboratory strain AD169 at an MOI of 3. At 24
835 hpi RNA was isolated with Trizol®, subsequently synthesized into cDNA via RT-PCR and
836 transcript levels assessed via SYBR Green PCR. The relative *SPOC1* mRNA levels were
837 calculated by normalization against housekeeping gene *RPL13A* (Biomol, Hamburg,
838 Germany). Statistical analysis was performed with Student's *t* test. Densitometric analysis
839 was performed with the AIDA Image Analyzer v.4.22 software and SPOC1 band
840 intensities at 24 hpi normalized against their corresponding β -actin signals. (C, D) HFF (C)
841 or ARPE-19 cells (D) were infected with the clinical isolate TB40/E at an MOI of 3 and
842 treated as described in (A). (E) Mouse embryonic fibroblasts (MEF) were infected with
843 MCMV at an MOI of 3, whole-cell lysates harvested throughout the replication cycle and
844 treated as described in (A). Immunoblotting was performed with the rat monoclonal
845 SPOC1 antibody and the monoclonal mouse-gB antibody. For all experiments monoclonal
846 antibody AC-15 (β -actin) served as a loading control.

847 **Figure 2. SPOC1 is a labile protein which is not upregulated by a viral tegument or**
848 **late protein.**

849 HFF cells were infected with AD169 (MOI 3) and in parallel treated with 150 $\mu\text{g/ml}$ CHX
850 (A) or with the proteasome inhibitor MG132 at 5 μM (B). The cells were harvested at
851 indicated time points; total-cell extracts were prepared, and subjected to SDS-PAGE and
852 immunoblotting. The used antibodies were directed against SPOC1 (α -SPOC1 rat), the
853 viral immediate-early protein IE1 (mAb p63-27), and in (A) the abundant tegument protein
854 pp65 (mAb 65-33) (C) HFF cells were infected with wt AD169 and UV-inactivated AD169
855 at a MOI of 3. Cells were then treated as described in (A). The used antibodies were
856 directed against SPOC1 and IE1 (D) HFFs were infected with wt AD169 at an MOI of 3
857 and in parallel with virus inoculation, 250 μM phosphonoformic acid (PFA) was added as
858 indicated to the infected-cell sample. Cells were harvested at 72 hpi; total-cell extracts were
859 prepared and subjected to SDS-PAGE and immunoblotting. The used antibodies were
860 directed against SPOC1, IE1, and the viral late protein MCP (mAb 28-4), serving as a
861 positive control for block of true late gene expression. For all experiments monoclonal
862 antibody AC-15 (β -actin) served as a loading control.

863 **Figure 3. The immediate early protein IE1 induces the upregulation of SPOC1.**

864 (A) SPOC1 expression levels were analyzed in doxycycline-treated and untreated HFF-
865 IE1 cells by Western blotting. IE1 expression was induced by treatment with 500 ng/ml
866 doxycyclin (Dox) for two different time intervals (24 h or 48 h). Cells were harvested;
867 total-cell extracts were prepared, separated by SDS-PAGE and subjected to
868 immunoblotting. The used antibodies were directed against SPOC1, the viral immediate-

869 early protein IE1 and the cellular protein PML (pAb A167+A168) as a control. (B) HFF
870 cells were infected with wt AD169, AD169 Δ IE1 and AD169/IE1-L174P at an MOI of 2.
871 Cells were harvested at indicated times post infection; total-cell extracts were prepared,
872 and subjected to SDS-PAGE and immunoblotting. The used antibodies were directed
873 against SPOC1, the viral immediate-early proteins IE1 (mAb p63-27) and IE2 (pHM 178),
874 and the viral early protein UL44 (mAb BS510). (C) Determination of SPOC1 half-life in
875 presence and absence of IE1 using cycloheximide (CHX) in doxycycline-treated (+Dox)
876 and untreated (-Dox) HFF-IE1 cells. 24 hours after induction of IE1 expression with
877 doxycycline, cells were treated with 25 μ g/ml of CHX and harvested at the indicated times
878 to assess SPOC1 expression levels by Western blot. (D) Densitometric analysis of (C) was
879 performed with the AIDA Image Analyzer v.4.22 software and SPOC1 band intensities
880 normalized against their corresponding β -actin signals. For all experiments monoclonal
881 antibody AC-15 (β -actin) served as a loading control.

882 **Figure 4. SPOC1 decline at late stage of HCMV infection is mediated by GSK-3 β .**

883 (A) HEK293T and HFF cells were treated with the GSK-3 β inhibitor LiCl and/or the
884 proteasome inhibitor MG132 for 6 h. Afterwards cells were harvested, lysed and subjected
885 to Western blot analysis with subsequent detection of SPOC1 expression levels. (B) Cell
886 lysates from Fig. 1C were analyzed for GSK-3 β expression using the polyclonal α -GSK-
887 3 β H-76 antibody. (C) HFF cells were infected with clinical isolate TB40/E at an MOI of
888 3 and in parallel treated with 40 μ M LiCl at 1.5 hpi (*) or 48 hpi. Cells were harvested at
889 96 hpi, total-cell extracts were prepared, separated by SDS-PAGE and subjected to
890 immunoblotting. (D) ARPE-19 cells were infected with TB40/E (MOI 3) and treated at 48

891 hpi with GSK-3 β inhibitors LiCl (40 μ M), SB-216763 (3 μ M; Sigma-Aldrich,
892 Deisenhofen, Germany), CHIR99021 (3 μ M; Tocris Bioscience, Wiesbaden-Nordenstadt,
893 Germany), and DMSO as a control. At 96 hpi cells were harvested, lysed and subjected to
894 Western blot analysis with subsequent detection of SPOC1 expression levels and the viral
895 late protein MCP (mAb 28-4) and pp28 (mAb 41-18) serving as a control for completion
896 of the HCMV replication cycle. For all experiments monoclonal antibody AC-15 (β -actin)
897 served as a loading control.

898 **Figure 5. Generation of HFF cells with a stable SPOC1 overexpression.**

899 (A) Western blot analysis for detection of SPOC1 in lysates of control (HFF/control) and
900 SPOC1-overexpressing HFFs (HFF/SPOC1) using an antibody against endogenous
901 SPOC1 (α -SPOC1 rat). (B) Immunofluorescence staining of SPOC1 in HFF/control and
902 HFF/SPOC1, using the mAb SPOC1 antibody. Cell nuclei were counterstained with DAPI
903 (4',6-diamidino-2-phenylindol).

904 **Figure 6. SPOC1 overexpression restricts initiation of IE gene expression.**

905 (A) HFF/SPOC1 and control HFF cells were either not infected (mock) or infected with
906 AD169 at a MOI of 1, and harvested at indicated times for Western blotting. Expression
907 kinetics of viral immediate-early protein IE1, viral early proteins (pUL84, pUL44, pUL97,
908 pp71), and viral late proteins (pp28, MCP) were compared. (B) Densitometric analysis
909 from (A) was performed with the AIDA Image Analyzer v.4.22 software. (C) Multistep
910 growth curve analyses of AD169 on HFF/control and HFF/SPOC1 cells. Cells were
911 infected with AD169 as indicated at a MOI of 0.005, 0.001, 0.0005, cell supernatants
912 harvested at indicated times post infection and analyzed for genome equivalents by HCMV

913 IE1-specific quantitative real-time PCR. (D) HFF/control and HFF/SPOC1 cells were
914 infected with HCMV laboratory strain AD169 at a MOI of 0.01. At 8 hpi intracellular DNA
915 was isolated and genome equivalents assessed via Taqman PCR in relation to albumin copy
916 numbers. (E) Analysis of IE gene expression in SPOC1 overexpressing cells with AD169
917 and TB40/E. HFF/control and HFF/SPOC1 cells were grown on coverslips in six-well
918 dishes, infected with 100 IEU/well of either laboratory strain AD169 or clinical isolate
919 TB40/E and fixed at 24 hpi. The number of IE-expressing cells was determined by indirect
920 immunofluorescence analysis using the monoclonal antibody p63-27 against the viral
921 protein IE1. Statistical analysis was performed with Student's *t* test.

922 **Figure 7. SPOC1 overexpression during the first hours of HCMV infection is vital for**
923 **efficient restriction.**

924 (A) Western blot analysis of the inducible HFF/SPOC1 (Tet-On) cells in presence (8 h, 16
925 h, 24 h) or absence (mock) of doxycycline. (B) Immunofluorescence analysis for detection
926 of SPOC1 in HFF/SPOC1 (Tet-On) cells in presence (+Dox, 24 h) or absence (-Dox) of
927 doxycycline. (C) HFF/SPOC1 (Tet-On) cells were treated with doxycycline for 24 h
928 (+Dox) or not treated (-Dox) as control and subsequently infected with HCMV laboratory
929 strain AD169 at a MOI of 0.001. At 8 hpi total RNA was isolated with Trizol, synthesized
930 into cDNA via RT-PCR and *IE1* transcript levels were assessed via Taqman PCR. The
931 relative *IE1* mRNA levels were calculated by normalization against albumin. (D) For
932 analysis of IE gene expression in HFF/SPOC1 (Tet-On) cells were grown on coverslips in
933 six-well dishes, while SPOC1 overexpression was induced by addition of doxycycline
934 (Dox) at different times prior (-24 h), in parallel (0 h) and post infection (+8 h) with 100

935 IEU/well of AD169 (schematically depicted with the timeline underneath). Cells were
936 fixed at 24 hpi and the number of IE-expressing cells determined by indirect
937 immunofluorescence analysis using the monoclonal antibody p63-27 against the viral
938 protein IE1. Statistical analysis was performed with Student's *t* test. (E) Multistep growth
939 curve analyses of AD169 on HFF/SPOC1 (Tet-On) cells in Dox presence (24 h prior to
940 infection) and Dox absence. Cells were infected with AD169 at an MOI of 0.001, cell
941 supernatants harvested at indicated times post infection and analyzed for genome
942 equivalents by HCMV IE1-specific quantitative real-time PCR.

943 **Figure 8. SPOC1 overexpression completely abrogates the onset of viral IE gene**
944 **expression.**

945 HFF/SPOC1 (Tet-On) cells were seeded in live-cell imaging chamber slides and SPOC1
946 overexpression was induced with doxycycline 24 hours prior to infection with the
947 recombinant reporter virus TB40/E-IE-mNeonGreen at an MOI of 0.05. In parallel,
948 untreated cells (-Dox) were used as control. For visualization of cell nuclei, SiR-DNA
949 (Spirochrome AG, Stein am Rhein, Germany) was added 2 hours prior to infection.
950 Infection was followed in real time, while images of 5 fields per condition were acquired
951 every 15 min for up to 30 hours. (A) The acquired stacks of time series for all fields were
952 automatically analyzed using an ImageJ macro. Solid lines display a three-point average
953 smoothing of the IE-mNeonGreen signal from 5 fields, with standard deviations of the
954 average. (B) Scatter dot plots show the distribution of signal onset in each field of control
955 (-Dox) and SPOC1 overexpressing HFFs (+Dox (-24 h)). Statistical analysis was
956 performed with an unpaired nonparametric *t* test (Mann-Whitney test). (C) Representative

957 images taken from the time series (5 to 30 hpi). (D, E) Manual single cell tracking was
958 performed with ImageJ and data sets analyzed by GraphPad Prism 6. After analyzing the
959 area under curve the first x corresponds to the onset of IE gene expression (D). The
960 maximal rate of gene expression was assessed by logistic growth curve fitting and
961 subsequently calculating the incline at its inflection point (E). Statistical analysis was
962 performed with an unpaired nonparametric *t* test (Mann-Whitney test).

963 **Figure 9. More cells initiate viral IE gene expression in the absence of SPOC1.**

964 (A, B) Endogenous SPOC1 level were either diminished by stable *SPOC1* knockout using
965 the CRISPR/Cas9 system, generated via lentiviral transduction and yielding in control
966 (HFF/CRISPR) and SPOC1 knockout HFFs (A) or by siRNA-mediated transient
967 transfection using 100 pmol of ON-Target plus human PHF13 (Dharmacon, Lafayette, CO,
968 USA) with two control siRNAs (#1 and #3) (B). Western blot analyses of endogenous
969 SPOC1 were performed to ensure efficient SPOC1 depletion. (C, D) Analysis of IE gene
970 expression in the absence of SPOC1 with AD169. SPOC1-depleted and respective control
971 cells were grown on coverslips in six-well dishes, infected with 100 IEU/well of either
972 laboratory strain AD169 or clinical isolate TB40/E and fixed at 24 hpi. The number of IE-
973 expressing cells was determined by indirect immunofluorescence analysis using the
974 monoclonal antibody p63-27 against the viral protein IE1. Statistical analysis was
975 performed with Student's *t* test. (E, F) HFF/CRISPR and HFF/SPOC1-k.o. cells were
976 infected with HCMV laboratory strain AD169 at an MOI of 0.01 (E) or 1 (F). At 8 hpi total
977 RNA was isolated with Trizol®, synthesized into cDNA via RT-PCR and IE1 transcript
978 levels were assessed via Taqman PCR. The relative *IE1* mRNA levels were calculated by

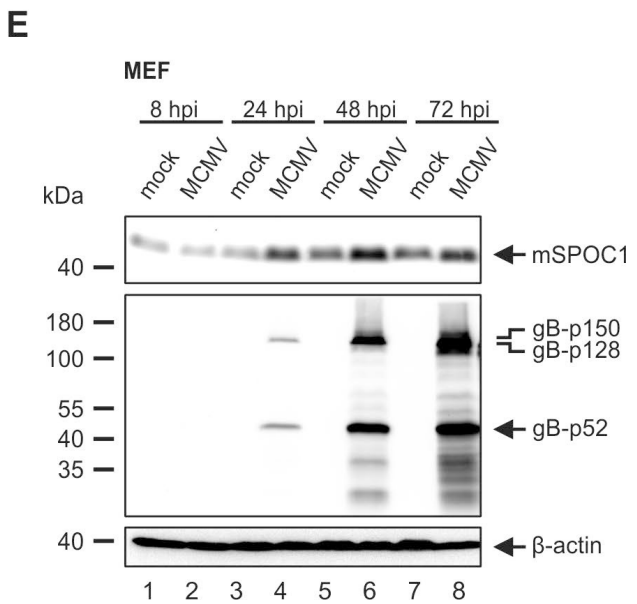
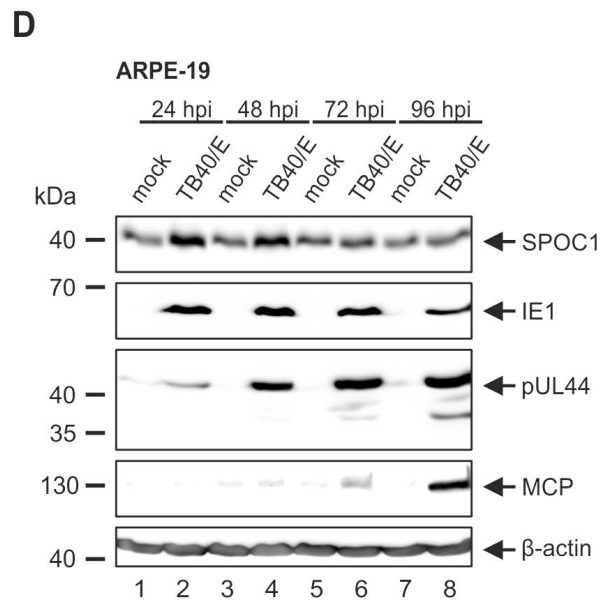
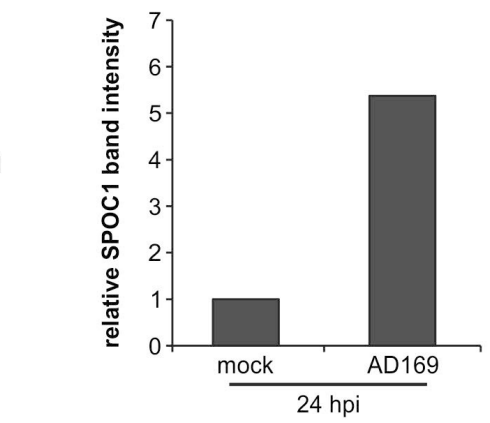
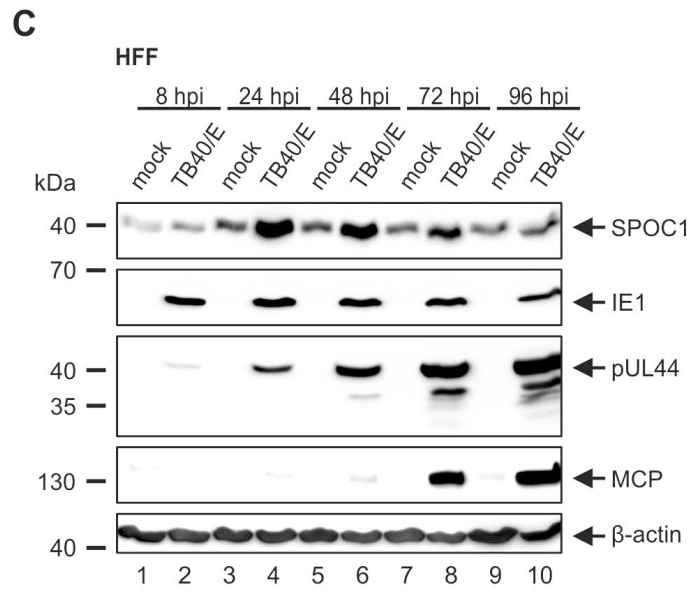
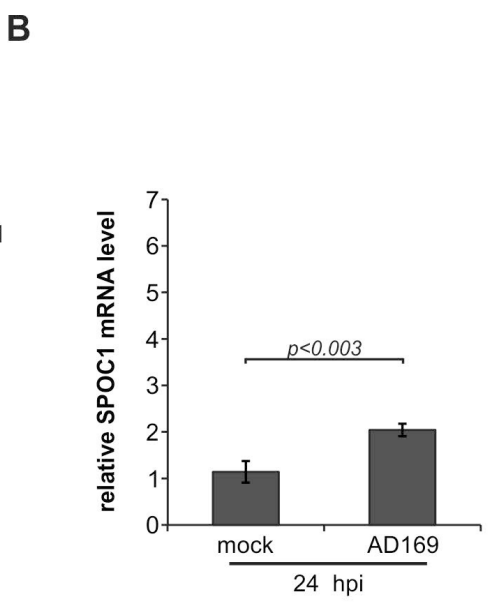
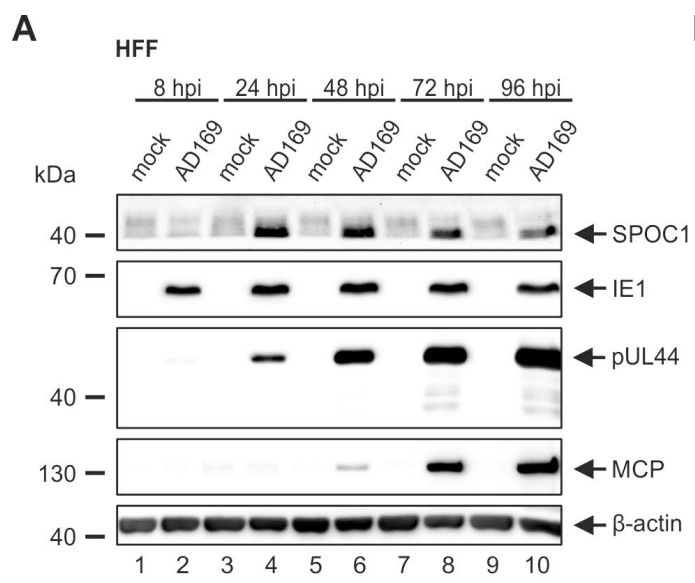
979 normalization against albumin. (G) Multistep growth curve analyses were conducted in
980 HFF/CRISPR and HFF/SPOC1-k.o. cells with wild-type AD169 (wt-AD169), or
981 recombinant mutant viruses deprived of either IE1 (AD169/del-IE1) or pp71 (AD169/del
982 pp71) (MOI of 0.001). Cell supernatants were harvested at indicated times post infection
983 and analyzed for genome equivalents by HCMV gB-specific quantitative real-time PCR.
984 Error bars indicate the standard deviation derived from three independent experiments.

985 **Figure 10. ChIP experiments reveal specific SPOC1 binding within the proximal**
986 **enhancer region of the major immediate-early promoter.**

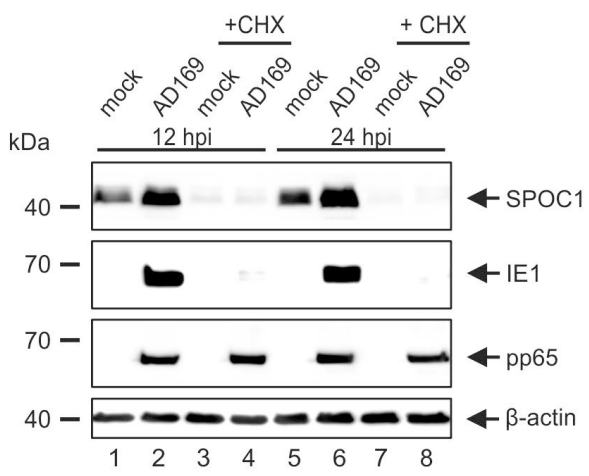
987 (A) Primary HFF cells were infected with TB40/E at an MOI of 0.5 and proteins cross-
988 linked 8 hpi and subsequent ChIP was performed with α -SPOC1 CR56 or α -HA as control.
989 After washing and elution, the samples were subjected to proteinase K digestion and
990 purified with the QIAquick MinElute PCR Purification Kit (Qiagen, Hilden, Germany).
991 Subsequently, samples were subjected to SYBRgreen qRT-PCR with primers targeting
992 different regions up- and downstream of the transcription start site (TSS) of the IE1 and
993 IE2 genes (regions shown relative to +1 of the TSS) (B) HFF/SPOC1 (Tet-On) cells were
994 induced with doxycycline (500 ng/ml) one day prior to infection with TB40/E (MOI 0.5).
995 8 hours post infection proteins were cross-linked and ChIP was performed with α -SPOC1
996 CR56. SPOC1 binding sites within the HCMV genome were mapped on the reference
997 sequence GenBank EF999921.1 Reads were deduplicated with samtools 1.3 and subjected
998 to peak-calling using the MACS2 IDR pipeline (C) Inset of the peak from (B) with depicted
999 open reading frames, the proximal and distal enhancer of the MIEP and the regions
1000 amplified by the primer pairs from (A).

Oligonucleotides used for cloning	
SPOC1_PacI_fw	CATATTAATTAATGGACTCTGACTCTTGCGCCG
SPOC1_EcoRI_rev	CATAGAATTCTCAGTCCAGGAACAGCTTCC
F-SPOC1 NotI	CATAGCGGCCGCATGGACTACAAAGACGATGA
EF1-alpha_ClaI_fw	CATAATCGATCCCGTCAGTGGGCAGAGCGC
3'EF1alpha-BamHI	CATAGGATCCTATTAGTACCAAGCTAATTC
SPOC1-fw-gRNA	CACCGCTCGTGGGGGTCTCCACGTA
SPOC1-rev-gRNA	AAACTACGTGGAGACCCCCACGAGC
Oligonucleotides used for qRT-PCR	
5'SPOC1	GACTCAGATGACGATTCTCTG
3'SPOC1	GGTGTGGCACTCATTACACTCG
+788_+732_fw	CCGCTGACGCATTTGGA
+788_+732_rev	CTCAGCTGCCTGCATCTTCTT
+39_-46_fw	GTGTACTATGGGAGGTCTAT
+39_-46_rev	AGGTCAAAACAGCGTGGATG
-1082_-1191_fw	AAGAAACACAAACGGCTGGATG
-1082_-1191_rev	TCGGCGACAGAAATCTCAAAAC

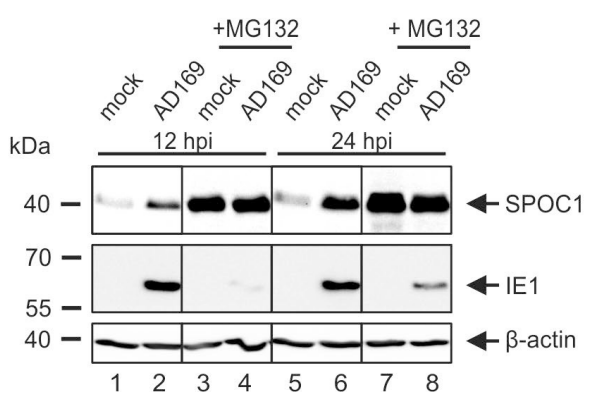
Table 1 Oligonucleotides used for plasmid construction and qRT-PCR.



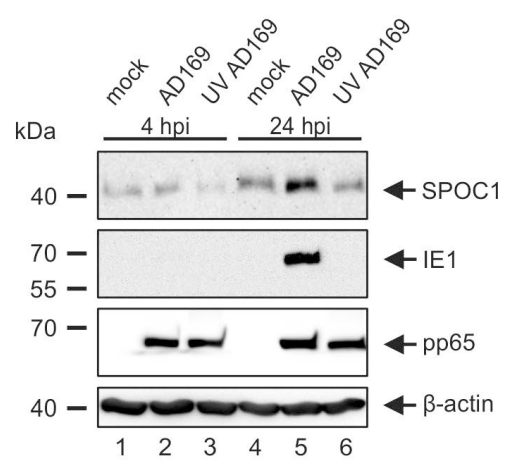
A



B



C



D

